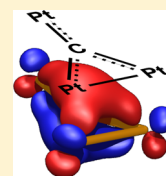


Unusual Bonding in Platinum Carbido Clusters

Dan J. Harding,^{†,‡,§} Christian Kerpel,[†] Gerard Meijer,[†] and André Fielicke^{*,†,||}[†]Fritz-Haber-Institut der Max-Planck-Gesellschaft, Faradayweg 4-6, D-14195 Berlin, Germany[‡]Institut für Physikalische Chemie, Georg-August-Universität Göttingen, Tammannstrasse 6, D-37077 Göttingen, Germany[§]Dept. of Dynamics at Surfaces, Max-Planck-Institut für biophysikalische Chemie, Am Fassberg 11, D-37077 Göttingen, Germany^{||}Institut für Optik und Atomare Physik, Technische Universität Berlin, Hardenbergstrasse 36, D-10623, Germany

Supporting Information

ABSTRACT: Vibrational spectroscopy and density functional theory calculations are used to determine the structures of small gas-phase platinum carbido clusters Pt_nC^+ , $n = 3-5$. The carbon atom is found to prefer three-coordinate binding sites near the center of the cluster, in contrast to most previously investigated adatoms on transition metal clusters. The Pt_3C unit is particularly stable, and binding of the carbon atom also leads to significant rearrangement of the metal framework when compared to the bare clusters.



SECTION: Spectroscopy, Photochemistry, and Excited States

The interaction and bonding of carbon atoms with transition metal atoms and surfaces is important in a number of areas including organometallic chemistry,¹ surface science,² and gas-phase cluster reactions.^{3,4} The interaction with platinum is particularly interesting because of its applications in heterogeneous catalysis. Significant efforts have been made to develop a microscopic understanding of the processes occurring in the coking of industrial catalysts⁵ and during the formation of graphene.⁶

Surprisingly, to our knowledge, the local binding geometries of carbon atoms adsorbed on platinum surfaces at low coverage are uncharacterized, in part because the formation of well-ordered low-coverage carbon layers is challenging.⁷ By contrast, the structures formed on single crystal surfaces at high carbon coverage have been studied extensively for a number of years.⁸ Additionally, real catalysts typically consist of small, disordered particles, which may have surface defects, steps and adatoms. Organometallic Pt–carbido cluster complexes, which could be useful models for Pt–C interactions, appear to be uncommon, although mixed metal carbido clusters, e.g., of Ru_nPt , are known.⁹ Platinum was thought not to form a stable carbide, but experiments have recently shown that PtC can be formed in a rock salt crystal structure at high pressure (85 GPa).¹⁰ Calculations suggest that the zinc blende crystal structure should be favored at low pressure while the rock salt structure observed in experiments is metastable and favored at high pressure.¹¹

Gas-phase clusters can provide tractable means to investigate the interactions of platinum and carbon in a controlled manner. Structures have been predicted for Pt_2C and Pt_3C^{2-} by Pyykkö et al., where they found that the carbon atom should sit in the center of the Pt atoms.¹² These structures are similar to CO_2 and the carbonate dianion, CO_3^{2-} , and they therefore suggested an “autogenic isolobal” structure of platinum and oxygen.^{12,13}

We have used infrared multiple photon dissociation (IRMPD) spectroscopy, with the rare-gas messenger atom

technique, to probe the structures of small platinum carbido clusters (Pt_nC^+ , $n = 3-5$). The experiments were performed at the Free Electron Laser for Infrared eXperiments (FELIX)¹⁴ at the FOM Institute for Plasma Physics Rijnhuizen in The Netherlands. The experimental setup and data analysis have been described in detail previously.^{15,16} Argon-tagged Pt_nC^+ clusters were generated by laser ablation of a ^{194}Pt target, with the resulting plasma cooled by a mix of Ar (0.1%) in He. A trace of CH_4 was added from a second valve situated on the cooled (173 K) thermalization channel. It appears that most of the Pt_nC^+ we observed was the product of reactions occurring in the ablation plasma. The total cluster intensity increased by a factor of 10 when CH_4 was added, suggesting that PtC acts as a nucleation center, promoting further cluster growth.

For all but the simplest systems, structure determination on the basis of IR spectroscopy requires comparison of the experimental spectrum with calculated spectra for different low-energy isomers. We used a two-step process to identify low energy isomers: candidate structures were found by basin-hopping Monte Carlo simulation,¹⁷ using density functional theory (DFT) at the BP86/def-SVP¹⁸⁻²⁰ level for the energy evaluation and local optimization. Our basin hopping program interfaces with TURBOMOLE,²¹ which performs the DFT calculations. These structures were reoptimized at the TPSS/def2-TZVP level,^{20,22,23} and their harmonic IR spectra were calculated. The argon tagging atoms were not included explicitly in the calculations, as they do not appear to strongly influence either the IR spectra in the frequency range we have investigated or the energetic ordering of the isomers. For the $Pt_4CAr_m^+$ system, we were able to measure spectra with good signal-to-noise for $m = 1-4$ in the region of the intense band at around 1000 cm^{-1} , and found that the band only shifts by

Received: February 4, 2013

Accepted: February 28, 2013

Published: February 28, 2013

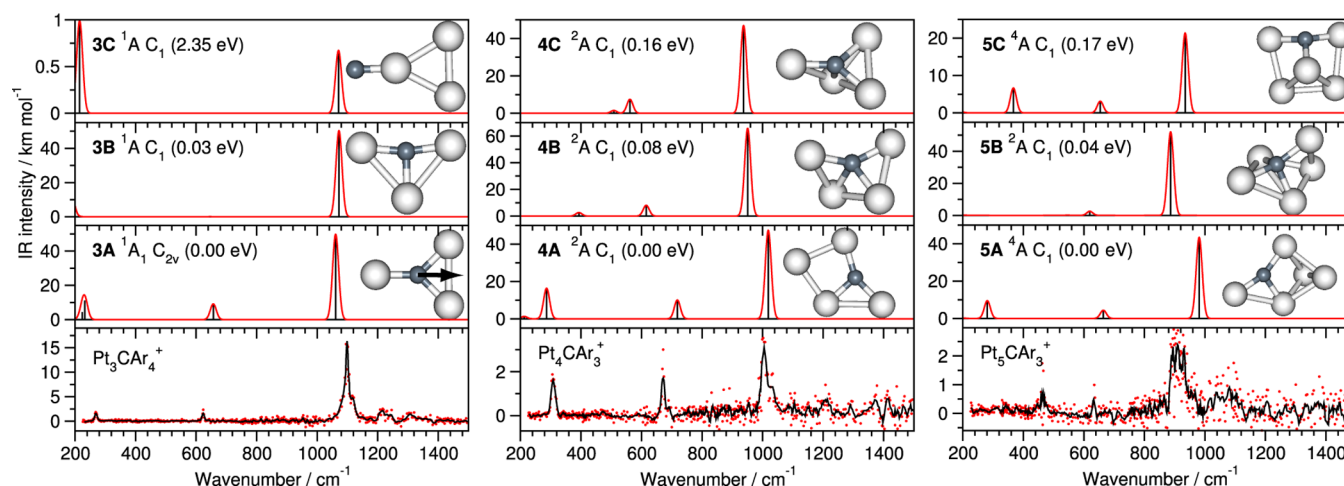


Figure 1. Comparison of experimental IRMPD spectra of argon-tagged Pt_nC^+ ($n = 3-5$) and calculated linear absorption spectra of low-energy isomers. The normal mode of the high frequency band in isomer 3A is also shown. The experimental cross sections are in arbitrary units. The calculated spectra are broadened with a Gaussian line shape of 20 cm^{-1} full width at half-maximum.

about $+20\text{ cm}^{-1}$ going from $m = 1$ to $m = 4$. We show the spectra for the clusters with high argon coverage as these provide the best signal-to-noise ratio, and these species are not populated by fragmentation of species with higher argon coverage. Details about our implementation of DFT basin hopping and Cartesian coordinates of all the structures are provided in the Supporting Information (SI).

Figure 1 shows the experimental IRMPD spectra for the argon complexes of Pt_nC^+ ($n = 3-5$) compared to the spectra of low-energy isomers of Pt_nC^+ calculated at the TPSS/def2-TZVP level of theory. The most notable feature of the IRMPD spectra is the high frequencies, around 1100 cm^{-1} , at which bands are observed. This is somewhat higher than the stretching frequency of the PtC molecule ($\omega_e = 1051.13\text{ cm}^{-1}$).²⁴ For other metal cluster carbide systems where vibrational frequencies have been determined, e.g., Nb_nC_m^- ^{25,26} or Al_3C^- ,²⁷ the highest fundamental frequencies, due to the metal–C modes, are around 800 cm^{-1} , suggesting that the binding of the carbon atom in Pt_nC^+ is significantly different.

The low energy structures found in the DFT calculations, shown in Figure 1, have the carbon atom near the center of the cluster. The calculated spectra of the lowest-energy isomers are a good match to the experimental spectra. We have also found higher energy isomers with the C in bridge and atop positions. While the highest frequency for the bridge site is too low (ca. 750 cm^{-1}), the atop structures have a band above 1000 cm^{-1} , which is reasonably close to that observed in the experiment. However, they have no features in the $500-700\text{ cm}^{-1}$ range where we also observe bands.

For Pt_3C^+ we find bands at 269, 623, 1098, and 1219 cm^{-1} . The best match to experiment is provided by a planar, C_{2v} symmetry structure (3A) with the carbon atom in the center of the molecule. A second low-energy structure (3B, 0.03 eV) is formed by the collapse of bridge bound input structures and also has the carbon near the center of the cluster. Carbon bound in an atop site (3C) might also explain the high frequency mode at 1098 cm^{-1} , but this structure is much higher in energy (2.35 eV). Neither 3B nor 3C are a good match to the experiment, as they have no IR active modes in the region around 600 cm^{-1} . The weak band at 1219 cm^{-1} is probably a van der Waals sideband, caused by exciting a combination of

Pt–C and Pt–Ar modes.^{28,29} The spacing of 121 cm^{-1} to the intense band is consistent with the Pt–Ar frequency we observed in Pt_nAr_m^+ complexes.³⁰ The high frequency band in isomer 3A is due to an a_1 , in plane, motion of the carbon atom along the symmetry axis of the molecule, which is illustrated by the arrow in the image of 3A shown in Figure 1.

Pyykkö et al. predicted that the dianion Pt_3C^{2-} should be a D_{3h} symmetric molecule with the carbon atom at the center. This is qualitatively similar to the structure we identify, and the differences in symmetry are probably due to the different charge states. A similar C_{2v} symmetric structure has been observed³¹ for neutral CO_3 (CO_3 has been studied in much less detail than the neutral), providing support both for the assumption that the geometric changes are due to the different charge states and also for the isolobality of Pt and O.

In an effort to explain why such high frequencies are observed, we have used natural bonding orbital (NBO) analysis and natural resonance theory (NRT)³² from calculations in NWChem 5.1³³ to investigate the bonding in the Pt_3C^+ cluster. The most important resonance structures, shown in Figure 2,

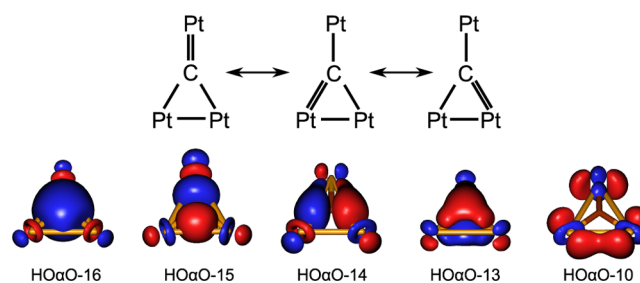


Figure 2. Leading configurations found in the NRT analysis and α -spin bonding molecular orbitals of Pt_3C^+ . The orbitals are labeled from the highest occupied alpha orbital (HO α O).

have three σ -bonds between the carbon atom and the platinum atoms, one σ -bond between a pair of platinum atoms, and an additional π -bond between the carbon and one of the platinum atoms. Each resonance structure has a weight of around 15%, while another 10 structures, with different σ -bond arrangements, contribute at least 3% each. The weights are very sensitive to the details of the calculation (i.e., symmetry of the

wave function, number of states used in the resonance analysis) but demonstrate a delocalization of the π -bond over the cluster. Figure 2 also shows the α -spin bonding molecular orbitals. The delocalization of the π -bond is clearly seen here, in HO α O-13, while a degree of delocalization is also seen in the σ -like HO α O-14 and HO α O-16. The other orbitals (not shown) are localized Pt lone pairs. The Pt–C bond lengths we find, 1.80 Å and 1.85 Å, are also consistent with partial double bonds: they are slightly longer than would be expected for a double bond based on the covalent double bond radii of platinum (1.12 Å) and carbon (0.67 Å).³⁴ The high frequency of the vibration then appears to be due to the high total bond order in the cluster rather than one, very stiff, multiple bond.

The lowest-energy structure (4A) we have found for Pt₄C⁺ is similar to isomer 3A with the extra platinum atom capping one of the Pt–C–Pt edges. The calculated spectrum of 4A is a good match to the experiment, matching the features at 308, 671, and 1006 cm⁻¹. The spectra of the other low-energy isomers (4B, 4C) do not compare so well, lacking the intense band at 308 cm⁻¹. The small energy difference between 4A and 4B suggests that both could be present in the cluster distribution; it is possible that we have observed only 4A because it forms complexes with Ar more efficiently.

For Pt₃C⁺ we find features centered at 463, 635, and 912 cm⁻¹. Again, the lowest-energy structure (5A) is based on the structure of 3A, now with a dimer capping one of the Pt–C–Pt edges. The spectrum of this isomer provides a reasonable match to the position of the main intense band at 912 cm⁻¹ and can also explain the very weak feature at 635 cm⁻¹. The calculated spectra of isomers 5B and 5C are rather similar to that of 5A which, when combined with the small energy differences between the isomers and the width of the main band in the experiment, means we are unable to determine whether one or multiple isomers are present in the molecular beam. The weak band at 463 cm⁻¹ is not well matched by the spectra of any of the low-energy isomers. The similarity of the experimental spectrum to those of the smaller sizes suggests that even if we have not found the lowest-energy structure, it contains a similar geometric motif.

The bonding between carbon and multiple platinum atoms results in rather strong interactions compared to most adatoms on clusters.³⁵ Table 1 shows the calculated binding energies per atom (E_b) and adsorption energies of carbon (E_{ads}) for different cluster sizes and comparison with the results of Viñes et al. for carbon adsorption on large clusters and on the Pt(111) surface.⁶ For completeness we also include the smallest carbides, PtC⁺ and Pt₂C⁺. Pt₂C⁺, shown in the SI, favors a

linear geometry like its neutral counterpart. The largest E_{ads} are found for Pt₂C⁺ and Pt₃C⁺, both around -8.6 eV, 1 eV more favorable than for Pt₅C⁺ and between 1.3 and 1.9 eV greater than for the favored 3-fold face-centered cubic (fcc) sites on the bulk models.

Table 1 also shows the comparison of the binding energy per atom, E_b , for pure platinum and platinum carbide clusters with a fixed total number of atoms, i.e., Pt_{*n*+1}⁺ and Pt_{*n*}C⁺. The pure platinum clusters have E_b in the range from -1.9 to -3.3 eV and become stronger bound with increasing cluster size. The carbides are more strongly bound, by as much as 1.5 eV per atom for $n = 2$ with the maximum in $|E_b|$ of 4.11 eV at the same size. This demonstrates both the enhanced binding in the PtC systems compared to the pure Pt clusters and the relative stability of the Pt₂C⁺ and Pt₃C⁺ units. Viñes et al. reported that relaxation of the platinum lattice was an important contribution to the binding energies, particularly for the cluster model when compared to the periodic Pt(111) calculations. In the small clusters, the binding of carbon also leads to significant structural changes when compared to the bare platinum clusters,³⁰ apparently driven by the formation of the delocalized Pt–C bonding network.

The structures of small Pt_{*n*}C⁺ clusters are significantly different from those found for nanocarbons of other transition metals. In the Nb₆C⁻ anion, the C atom has been found to occupy a hollow site.²⁶ In neutral Nb₃C, carbon occupies a bridge site, while larger clusters and higher carbon coverage favor hollow sites.^{25,36} Similar changes in binding site are reported for tantalum clusters, Ta₃C and Ta₄C, favoring bridge sites, while higher carbon coverage leads to hollow site binding.^{37,38} Al₃C has been reported to have a C_{2v} symmetry Y-shaped structure²⁷ similar to Pt₃C⁺. The presence of the carbon atom, and its preference for a site in the center of the Pt clusters, leads to much greater distortion of the metal cluster than has been observed for other transition metal cluster–adatom systems. The adsorption of oxygen on Ta clusters leads to only small distortion of the underlying metal cluster,²⁹ while in Pt_{*n*}O_{*m*}⁺ systems, the geometry of the metal cluster is changed (from 3D to 2D for $n = 4,5$) but the Pt atoms remain directly connected.^{30,39}

In conclusion, we have determined the structure of small platinum carbido clusters, finding the carbon atom to prefer sites near the center of the cluster and inducing significant rearrangement of the underlying cluster structure. The apparent stability of these structures is surprising given the low solubility of carbon in bulk platinum and the lack of organometallic compounds with platinum-carbido bonds. Similar structures might be formed following carbon adsorption on rough platinum surfaces, and the high relative stability of the Pt₂C and Pt₃C units suggests it may be possible to synthesize related compounds using chemical methods.

Table 1. Calculated Binding Energies in Pt_{*n*}C⁺ Clusters^a

<i>n</i>	E_{ads}/eV	$E_b(\text{Pt}_n\text{C}^+)/\text{eV}$	$E_b(\text{Pt}_{n+1}^+)/\text{eV}$
1	-4.70	-2.35	-1.89
2	-8.57	-4.11	-2.54
3	-8.59	-4.06	-3.28
4	-6.94	-4.01	-3.28
5	-7.54	-3.99	
C on Pt ₇₉ ^b	-7.33		
C on Pt(111) 1/16 ML ^b	-6.71		

^aThe binding energy per atom (E_b) is calculated as $(E_{\text{Pt}_n\text{C}^+} - E_{\text{Pt}_n^+} - (n - 1) \cdot E_{\text{Pt}} - E_{\text{C}})/(n + 1)$. The adsorption energy (E_{ads}) of carbon is $E_{\text{Pt}_n\text{C}^+} - (E_{\text{Pt}_n^+} + E_{\text{C}})$. $E_{\text{Pt}_n^+}$ is for the isomers and energies determined in ref 29. ^bViñes et al. (ref 6).

■ ASSOCIATED CONTENT

📄 Supporting Information

Details of the DFT basin hopping, the Pt₂C⁺ system, and the Cartesian coordinates for all of the structures described here. This material is available free of charge via the Internet at <http://pubs.acs.org>.

■ AUTHOR INFORMATION

Corresponding Author

*E-mail: fielicke@physik.tu-berlin.de.

Notes

The authors declare no competing financial interest.

ACKNOWLEDGMENTS

We gratefully acknowledge the support of the Stichting voor Fundamenteel Onderzoek der Materie (FOM) for providing FELIX beam time and the FELIX staff, in particular Dr. B. Redlich and Dr. A.F.G. van der Meer, for their skillful assistance. This work is supported by the Deutsche Forschungsgemeinschaft through research Grant FI893/3-1. DJH thanks the Alexander-von-Humboldt-Stiftung for support.

REFERENCES

- (1) Takemoto, S.; Matsuzaka, H. Recent Advances in the Chemistry of Ruthenium Carbido Complexes. *Coord. Chem. Rev.* **2012**, *256*, 574–588.
- (2) Deng, R.; Herceg, E.; Trenary, M. Identification and Hydrogenation of C₂ on Pt(111). *J. Am. Chem. Soc.* **2005**, *127*, 17628–17633.
- (3) Achatz, U.; Berg, C.; Joos, S.; Fox, B. S.; Beyer, M. K.; Niedner-Schatteburg, G.; Bondybey, V. E. Methane Activation by Platinum Cluster Ions in the Gas Phase: Effects of Cluster Charge on the Pt₄ Tetramer. *Chem. Phys. Lett.* **2000**, *320*, 53–58.
- (4) Harding, D. J.; Kerpel, C.; Meijer, G.; Fielicke, A. Activated Methane on Small Cationic Platinum Clusters. *Angew. Chem., Int. Ed.* **2012**, *51*, 817–819.
- (5) Paäl, Z.; Wootsch, A.; Matusek, K.; Wild, U.; Schlögl, R. Intentional Carbonization of Pt Black: A Model Spectroscopic and Catalytic Study. *Catal. Today* **2001**, *65*, 13–18.
- (6) Viñes, F.; Neyman, K. M.; Görling, A. Carbon on Platinum Substrates: From Carbodic to Graphitic Phases on the (111) Surface and on Nanoparticles. *J. Phys. Chem. A* **2009**, *113*, 11963–11973.
- (7) Smirnov, M. Y.; Gorodetskii, V. V.; Cholach, A. R.; Zemlyanov, D. Y. Hydrogenation of Isolated Atoms and Small Clusters of Carbon on Pt(111) Surface: HREELS/TDS Studies. *Surf. Sci.* **1994**, *311*, 308–321.
- (8) Lang, B. A LEED Study of the Deposition of Carbon on Platinum Crystal Surfaces. *Surf. Sci.* **1975**, *53*, 317–329.
- (9) Takemoto, S.; Morita, H.; Karitani, K.; Fujiwara, H.; Matsuzaka, H. A Bimetallic Ru₂Pt Complex Containing a Trigonal-Planar μ_3 -Carbido Ligand: Formation, Structure, and Reactivity Relevant to the Fischer–Tropsch Process. *J. Am. Chem. Soc.* **2009**, *131*, 18026–18027.
- (10) Ono, S.; Kikegawa, T.; Ohishi, Y. A High-Pressure and High-Temperature Synthesis of Platinum Carbide. *Solid State Commun.* **2005**, *133*, 55–59.
- (11) Sun, X.-W.; Chen, Q.-F.; Chen, X.-R.; Cai, L.-C.; Jing, F.-Q. First-Principles Investigations of Elastic Stability and Electronic Structure of Cubic Platinum Carbide under Pressure. *J. Appl. Phys.* **2011**, *110*, 103507.
- (12) Pyykkö, P.; Patzschke, M.; Suupere, J. Calculated Structures of [Au=C=Au]²⁺ and Related Systems. *Chem. Phys. Lett.* **2003**, *381*, 45–52.
- (13) Patzschke, M.; Pyykkö, P. Darmstadtium Carbonyl and Carbide Resemble Platinum Carbonyl and Carbide. *Chem. Commun.* **2004**, 1982–1982.
- (14) Oepts, D.; van der Meer, A. F. G.; van Amersfoort, P. W. The Free-Electron-Laser User Facility FELIX. *Infrared Phys. Technol.* **1995**, *36*, 297–308.
- (15) Fielicke, A.; Kirilyuk, A.; Ratsch, C.; Behler, J.; Scheffler, M.; von Helden, G.; Meijer, G. Structure Determination of Isolated Metal Clusters via Far-Infrared Spectroscopy. *Phys. Rev. Lett.* **2004**, *93*, 023401.
- (16) Fielicke, A.; von Helden, G.; Meijer, G. Far-Infrared Spectroscopy of Isolated Transition Metal Clusters. *Eur. Phys. J. D* **2005**, *34*, 83–88.
- (17) Wales, D. J.; Doye, J. P. K. Global Optimization by Basin-Hopping and the Lowest Energy Structures of Lennard-Jones Clusters Containing up to 110 Atoms. *J. Phys. Chem. A* **1997**, *101*, 5111–5116.
- (18) Becke, A. D. Density-Functional Exchange-Energy Approximation with Correct Asymptotic Behavior. *Phys. Rev. A* **1988**, *38*, 3098–3100.
- (19) Perdew, J. P. Density-Functional Approximation for the Correlation Energy of the Inhomogeneous Electron Gas. *Phys. Rev. B* **1986**, *33*, 8822–8824.
- (20) Weigend, F.; Häser, M.; Patzelt, H.; Ahlrichs, R. RI-MP2: Optimized Auxiliary Basis Sets and Demonstration of Efficiency. *Chem. Phys. Lett.* **1998**, *294*, 143–152.
- (21) Ahlrichs, R.; Bär, M.; Häser, M.; Horn, H.; Kölmel, C. Electronic Structure Calculations on Workstation Computers: The Program System TURBOMOLE. *Chem. Phys. Lett.* **1989**, *162*, 165–169.
- (22) Tao, J.; Perdew, J. P.; Staroverov, V. N.; Scuseria, G. E. Climbing the Density Functional Ladder: Nonempirical Meta-Generalized Gradient Approximation Designed for Molecules and Solids. *Phys. Rev. Lett.* **2003**, *91*, 146401.
- (23) Weigend, F.; Ahlrichs, R. Balanced Basis Sets of Split Valence, Triple Zeta Valence and Quadruple Zeta Valence Quality for H to Rn: Design and Assessment of Accuracy. *Phys. Chem. Chem. Phys.* **2005**, *7*, 3297–3305.
- (24) Appelblad, O.; Nilsson, C.; Scullman, R. Vibrational and Rotational Analysis of Some Band Systems of the Molecule PtC. *Phys. Scr.* **1973**, *7*, 65–71.
- (25) Yang, D.-S.; Zgierski, M. Z.; Bérces, A.; Hackett, P. A.; Roy, P.-N.; Martinez, A.; Tucker Carrington, J.; Salahub, D. R.; Fournier, R.; Pang, T.; Chen, C. Vibrational and Geometric Structures of Nb₃C₂ and Nb₃C₂⁺ from Pulsed Field Ionization-Zero Electron Kinetic Energy Photoelectron Spectra and Density Functional Calculations. *J. Chem. Phys.* **1996**, *105*, 10663–10671.
- (26) Haertelt, M.; Lapoutre, V. J. F.; Bakker, J. M.; Redlich, B.; Harding, D. J.; Fielicke, A.; Meijer, G. Structure Determination of Anionic Metal Clusters via Infrared Resonance Enhanced Multiple Photon Electron Detachment Spectroscopy. *J. Phys. Chem. Lett.* **2011**, *2*, 1720–1724.
- (27) Boldyrev, A. I.; Simons, J.; Li, X.; Chen, W.; Wang, L.-S. Combined Photoelectron Spectroscopy and Ab Initio Study of the Hypermetallic Al₃C Molecule. *J. Chem. Phys.* **1999**, *110*, 8980–8985.
- (28) Bakker, J. M.; Satink, R. G.; von Helden, G.; Meijer, G. Infrared Photodissociation Spectroscopy of Benzene–Ne, Ar Complex Cations. *Phys. Chem. Chem. Phys.* **2002**, *4*, 24–33.
- (29) Fielicke, A.; Gruene, P.; Haertelt, M.; Harding, D. J.; Meijer, G. Infrared Spectroscopy and Binding Geometries of Oxygen Atoms Bound to Cationic Tantalum Clusters. *J. Phys. Chem. A* **2010**, *114*, 9755–9761.
- (30) Harding, D. J.; Kerpel, C.; Rayner, D. M.; Fielicke, A. Communication: The Structures of Small Cationic Gas-Phase Platinum Clusters. *J. Chem. Phys.* **2012**, *136*, 211103.
- (31) Moll, N. G.; Clutter, D. R.; Thompson, W. E. Carbon Trioxide: Its Production, Infrared Spectrum, and Structure Studied in a Matrix of Solid CO₂. *J. Chem. Phys.* **1966**, *45*, 4469–4481.
- (32) Glendenning, E. D.; Badenhop, J. K.; Reed, A. E.; Carpenter, J. E.; Bohmann, J. A.; Morales, C. M.; Weinhold, F. NBO 5.G.; Theoretical Chemistry Institute, University of Wisconsin: Madison, WI, 2004; <http://www.chem.wisc.edu/nbo5>.
- (33) Bylaska, E. J.; de Jong, W. A.; Govind, N.; Kowalski, K.; Straatsma, T. P.; Valiev, M.; Wang, D.; Apra, E.; Windus, T. L.; Hammond, J. et al. *NWChem, A Computational Chemistry Package for Parallel Computers*, version 5.1.1; Pacific Northwest National Laboratory: Richland, WA; 2009.
- (34) Pyykkö, P.; Atsumi, M. Molecular Double-Bond Covalent Radii for Elements Li–E112. *Chem.—Eur. J.* **2009**, *15*, 12770–12779.
- (35) Rösch, N.; Petrova, G. P.; Petkov, P. S.; Genest, A.; Krüger, S.; Aleksandrov, H. A.; Vayssilov, G. N. Impurity Atoms on Small Transition Metal Clusters. Insights from Density Functional Model Studies. *Top. Catal.* **2011**, *54*, 363–377.
- (36) Dryza, V.; Addicoat, M. A.; Gascooke, J. R.; Buntine, M. A.; Metha, G. F. Threshold Photoionization and Density Functional

Theory Studies of the Niobium Carbide Clusters Nb_3C_n ($n = 1-4$) and Nb_4C_n ($n = 1-6$). *J. Phys. Chem. A* **2008**, *112*, 5582–5592.

(37) Dryza, V.; Addicoat, M.; Gascooke, J.; Buntine, M.; Metha, G. Ionization Potentials of Tantalum–Carbide Clusters: An Experimental and Density Functional Theory Study. *J. Phys. Chem. A* **2005**, *109*, 11180–11190.

(38) Dryza, V.; Alvino, J. F.; Metha, G. F. Onset of Carbon-Carbon Bonding in Ta_5C_y ($y = 0-6$) Clusters: A Threshold Photoionization and Density Functional Theory Study. *J. Phys. Chem. A* **2010**, *114*, 4080–4085.

(39) Kerpál, C.; Harding, D. J.; Hermes, A. C.; Meijer, G.; Mackenzie, S. R.; Fielicke, A. Structures of Platinum Oxide Clusters in the Gas Phase. *J. Phys. Chem. A* **2013**, *117*, 1233–1239.